

COVER SPALLING IN HSC COLUMNS LOADED IN CONCENTRIC COMPRESSION

By Stephen J. Foster,¹ Jing Liu,² and Shamim A. Sheikh³

ABSTRACT: Experimental studies on concentrically loaded high-strength reinforced-concrete columns have indicated that the cover spalls prior to the section reaching its squash load, if the squash load is calculated from the gross sectional area. To investigate the mechanics of cover spalling, specifically for high-strength reinforced-concrete columns but also for conventional-strength columns, a finite-element model is developed. Cover spalling is simulated by setting the elastic modulus of the cover elements to a low value once a threshold tension strain is reached at the cover-core interface, with the threshold tension strain chosen to match experimentally recorded axial strain data. Radial tension stresses exist at the cover-core interface due to restraint of the Poisson growth of the core provided by the ties. Increasing the volume of ties increases the restraint and increases the radial tension stress at the cover-core interface. Postanalysis revealed that the stress at the point of cover spalling matches well with the triaxial tension strength of the unreinforced cover. Analysis of experimental data reinforces the findings of the finite-element model. It is recommended that for reinforced columns cast from concrete with cylinder strengths greater than 60 MPa, the maximum load be taken as 0.85 times the capacity of the concrete section (based on the in-situ concrete strength) or the capacity of the confined core, whichever is greater, plus the capacity of the longitudinal reinforcement.

INTRODUCTION

Experimental studies on high-strength concrete (HSC) columns under concentric axial loading have shown that the strength is affected by spalling of the cover and the inability of the concrete core to carry increased loads after the cover is shed. In some studies, early cover spalling has been observed for columns with mean cylinder strengths as low as 66 MPa (Polat 1992; Foster and Attard 1997b). Various theories have been postulated for the observed behavior, including buckling of the cover shell (Paultre et al. 1996) and restrained shrinkage in the cover shell combined with shrinkage of the HSC around the reinforcing steel (Sundaraj and Sheikh 1992; Collins et al. 1993). In a finite-element (FE) study on concentrically loaded columns by Liu and Foster (1998a), it was shown that high tension strains exist between the cover-core interface at loads significantly below peak loads. While a proportion of this strain is due to the Poisson effect, and hence will not lead to stress cracking, a portion is also due to the restraint provided to the core by the tie reinforcement. The constrained core and unconstrained cover set up transverse tension stresses at the core-cover interface. Once significant tension strength across the interface is lost, the cover shell is free to buckle away from the core. Further evidence of this behavior is presented in the current paper.

The mechanics of cover spalling can be best understood by combining experimental observations with FE analyses. In addition to demonstrating that high tensile strains exist across the core-cover interface, Liu and Foster (1998a) also showed that at the peak load the tie reinforcement cannot be taken to have yielded. Similar observations have been made in a number of experimental studies (Cusson and Paultre 1994; Razvi and Saatcioglu 1996; Foster and Attard 1997a,b). The FE

model of Liu and Foster (1998a) is extended in the present paper to include the effects of cover spalling.

FINITE-ELEMENT MODELING OF TIED COLUMNS

Liu and Foster (1998a) developed an axisymmetric FE model for confined concrete members based on the explicit microplane formulation of Carol et al. (1992). The formulation divides each sample point into 28 microplanes over which the volumetric, deviatoric, and tangential material laws are numerically integrated. The material laws are given by

volumetric law

$$\sigma_v = E_v^0 \epsilon_v [(1 + |\epsilon_v|/a)^{-p} + (|\epsilon_v|/b)^q] \quad \text{for compression} \quad (1a)$$

$$\sigma_v = E_v^0 \epsilon_v e^{-(|\epsilon_v|/a_1)^{p_1}} \quad \text{for tension} \quad (1b)$$

deviatoric law

$$\sigma_D = E_D^0 \epsilon_D e^{-(|\epsilon_D|/a_2)^{p_2}} \quad \text{for compression} \quad (2a)$$

$$\sigma_D = E_D^0 \epsilon_D e^{-(|\epsilon_D|/a_2)^{p_2}} \quad \text{for tension} \quad (2b)$$

tangential law

$$\sigma_{Tr} = \tau \epsilon_{Tr} / \nu \quad (3a)$$

$$\tau = E_T^0 \nu e^{-(\nu/a_3)^{p_3}} \quad (3b)$$

where (σ_v, ϵ_v) , (σ_D, ϵ_D) , $(\sigma_{Tr}, \epsilon_{Tr})$ = volumetric, deviatoric, and shear stresses and strains, respectively; ν = Euclidean length of the transverse strain vector ($\nu = \sqrt{\epsilon_{Tr} \epsilon_{Tr}}$); and E_v^0 , E_D^0 , E_T^0 = initial volumetric, deviatoric, and tangential moduli, respectively.

The initial volumetric, deviatoric, and tangential moduli are given by

$$E_v^0 = \frac{E_0}{1 - 2\mu}, E_D^0 = \eta_0 E_v^0, E_T^0 = \frac{1}{3} \left[\frac{5(1 - 2\mu)}{1 + \mu} - 2\eta_0 \right] E_v^0 \quad (4)$$

where E_0 = initial modulus of elasticity; μ = Poisson's ratio; and η_0 ($\eta_0 = 1$ in the present study) = ratio of the initial deviatoric modulus to the initial volumetric modulus (E_D^0/E_v^0). The fixed parameters, a , b , p , and q , have the following values: $a = 0.005$, $b = 0.225$, $p = 0.25$, and $q = 2.25$ (Bazant and Prat 1988a,b) with p_1 also fixed at $p_1 = 0.55$. The parameters a_1 , a_2 , a_3 , p_2 , and p_3 are taken as functions of the major to minor principal stress ratio (σ_1/σ_3) and fitted with the cubic spline

¹Sr. Lect., School of Civ. and Envir. Engrg., The Univ. of New South Wales, Sydney, 2052, Australia.

²Res. Student, School of Civ. and Envir. Engrg., The Univ. of New South Wales, Sydney, 2052, Australia.

³Prof., Dept. of Civ. Engrg., Univ. of Toronto, Toronto, M5S 1A4, Canada.

Note. Associate Editor: Walter H. Gerstle. Discussion open until May 1, 1999. To extend the closing date one month, a written request must be filed with the ASCE Manager of Journals. The manuscript for this paper was submitted for review and possible publication on February 2, 1998. This paper is part of the *Journal of Structural Engineering*, Vol. 124, No. 12, December, 1998. ©ASCE, ISSN 0733-9445/98/0012-1431-1437/\$8.00 + \$.50 per page. Paper No. 17534.

$$q = s_0 + s_1(\sigma_1/\sigma_3) + s_2(\sigma_1/\sigma_3)^2 + s_3(\sigma_1/\sigma_3)^3 \quad (5)$$

where q = parameter being considered (a_1 , a_2 , a_3 , p_2 , or p_3); and s_0 , s_1 , s_2 , and s_3 = set of spline coefficients. A full set of spline coefficients for concrete strengths from 20 to 100 MPa are given in Liu and Foster (1998b). Sensitivity studies on the material laws by Liu and Foster found the model to be highly sensitive to the initial elastic modulus E_0 . The parameters used in the present study correspond to an initial elastic modulus given by $E_0 = 0.043\rho^{1.5}\sqrt{f'_c}$, where ρ is the concrete density in kg/m^3 .

SPALLING OF COVER

To study the behavior of the concrete cover region, a finite-element analysis was undertaken for the concentrically loaded circular column specimens CC-15 and CC-16 of Razvi and Saatcioglu (1996). The specimens were modeled using the axisymmetric FE meshes shown in Fig. 1. Mesh sensitivity studies for columns CC-15 and CC-16 were undertaken by Liu and Foster (1998b). The study showed the finite-element model to be relatively insensitive to the mesh grading. The finer of the meshes tested by Liu and Foster are used in the present study. To induce the localization at the centerline (Fig. 1), the hoop steel away from the centerline was increased over that used in the experiments. Cover spalling was included in the model by setting the cover elements to a low stiffness once a threshold tension strain was reached.

The concrete was modeled using eight-node isoparametric, axisymmetric elements with numerical integration over a 3×3 Gaussian quadrature. The microplane material parameters used to develop the stress-strain laws are shown in Fig. 2, and correspond to the experimentally obtained in-situ concrete strength of $f_{cp} = 83$ MPa, or $0.9 f'_c$. The importance of including the test rig arrangement in determining the "true" response of standard laboratory control specimens, such as those used to get the compression stress-strain curves, is identified by van Mier (1997). This is particularly true when studying the postpeak response. Bažant et al. (1996) points to the difficulty of decontaminating material parameters developed from laboratory test data where strain-softening localization exists, and note that it has typically been ignored. In the present study, the stress-strain curves obtained from cylinder tests are delocalized using a back-analysis technique. In this method, the elemental stress-strain relationships are obtained by numerically modeling a concrete cylinder with the strains measured over the full height of the cylinder. The correct elemental relationships are those that reproduce the results of the cylinder tests, including the volumetric changes. The stress-strain curves for analyses of 150 mm diameter \times 300 mm high concrete cylinders under various confining pressures, using the

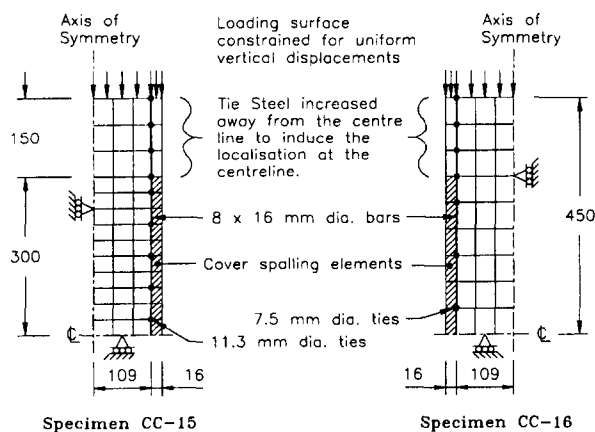


FIG. 1. FE Meshes for Razvi and Saatcioglu (1996) Specimens CC-15 and CC-16

microplane parameters given in Fig. 2, are shown in Fig. 3. Further details on the calibration of the numerical model, including the effect of localization on the "pure" elemental stress-strain response, are given in Liu and Foster (1998a,b).

In the analysis of circular reinforced-concrete columns, the ineffectively confined concrete within the core between ties is an important parameter and, thus, the tie steel needs to be modeled as discrete elements. The tie reinforcement was modeled using point elements with a trilinear stress-strain curve to closely match the experimental data (Fig. 4). Numerical difficulties caused by stress infinities arising from applying a point load to adjacent concrete elements were controlled by limiting the maximum change in the confinement ratio (σ_1/σ_3) between load steps and limiting the maximum σ_1/σ_3 at any

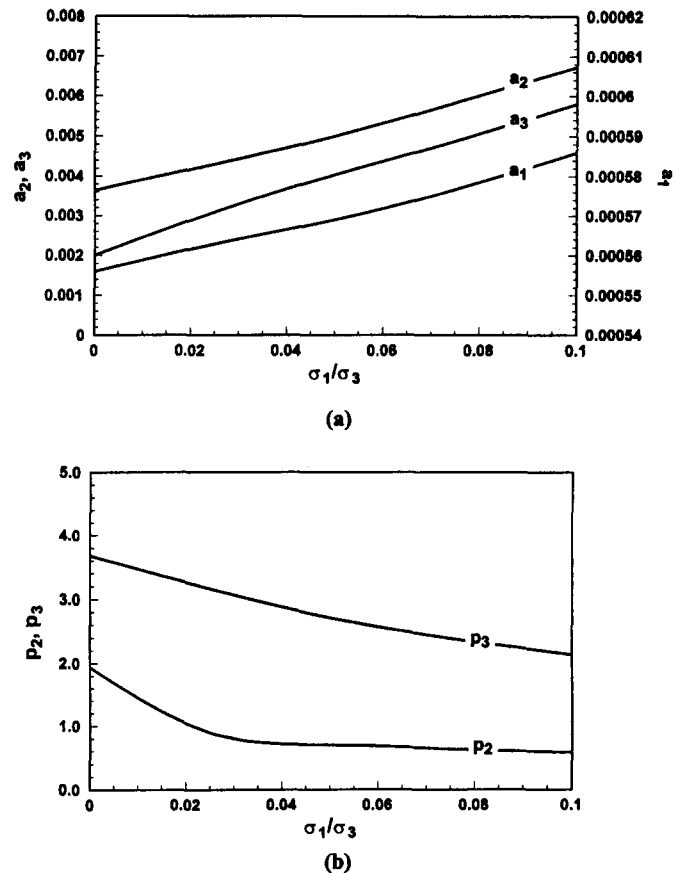


FIG. 2. Microplane Parameters versus Maximum to Minimum Principal Stress Ratio for $f_{cp} = 83$ MPa: (a) Parameters a_1 , a_2 , and a_3 ; (b) Parameters p_2 and p_3

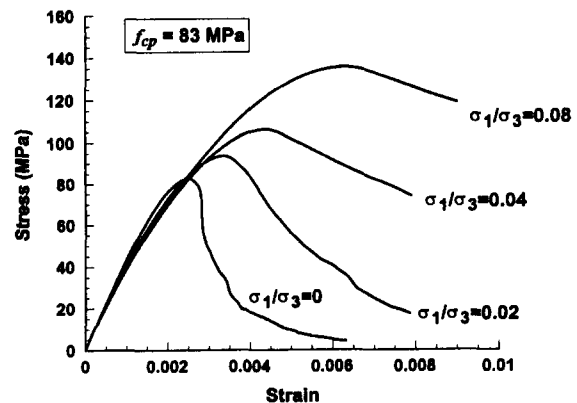


FIG. 3. Stress-Strain Curves for 150 mm Diameter \times 300 mm Concrete Cylinder under Varying Confining Pressures, Generated Using Microplane Parameters of Liu and Foster (1997a) for $f_{cp} = 83$ MPa

Gauss point to that predicted using the confinement model discussed later. Numerical tests were undertaken to ensure the results were unaffected by the limitations imposed with small displacement steps (0.005 ~ 0.01 mm) used from the point of cover spalling to beyond the peak.

The longitudinal steel was modeled using three-node bar elements with the elemental stiffness matrix obtained using numerical integration on a two-point Gauss quadrature. An elastic perfectly plastic stress-strain law was used for the longitudinal reinforcement with a yield stress of 450 MPa. The initial elastic modulus for both the tie and the longitudinal reinforcement was taken as 200 GPa.

In the experimental columns of Razvi and Saatcioglu, axial strains were measured over a gauge length of 300 mm or a half length of 150 mm measured from the centerline (Fig. 1). The results of the numerical analyses are shown in Figs. 5(a)

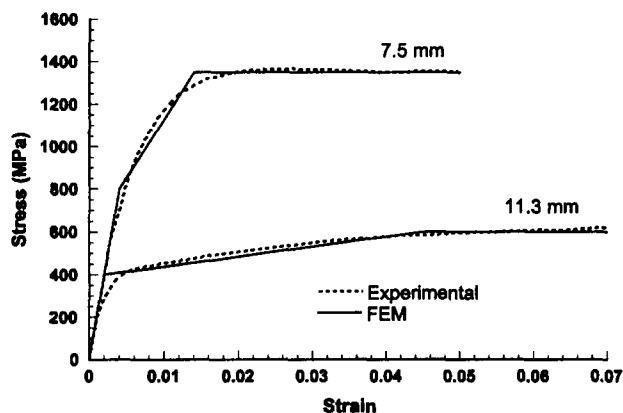


FIG. 4. Stress-Strain Curves for Ties Used in Razvi and Saatcioglu (1996) Columns

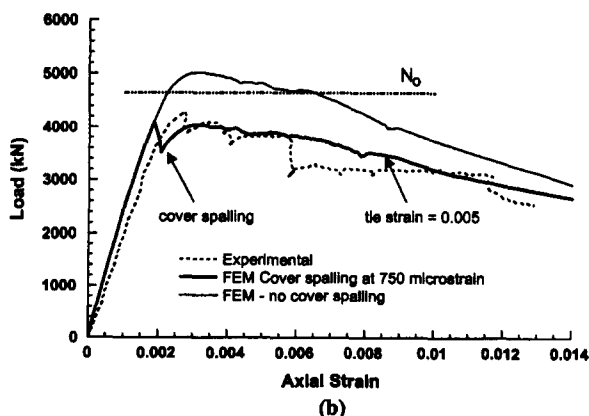
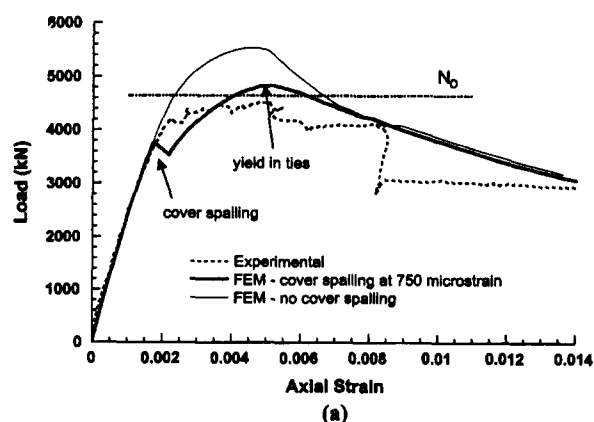


FIG. 5. FE Analyses of Razvi and Saatcioglu (1996) Columns, with and without Cover Spalling, for Specimens: (a) CC-15; (b) CC-16

and 5(b) for specimen CC-15 and specimen CC-16, respectively, for strains measured over a half gauge length of 150 mm. A good correlation is seen between the numerical and experimental results, especially when cover spalling is included in the model. For the cover spalling, the best match was obtained for a threshold spalling strain of 750 $\mu\epsilon$.

Collins et al. (1993) suggested that the early cover spalling observed in HSC columns is possibly due to differential drying shrinkage between the core and the cover shell leading to a cracking plane. Cusson and Paultre (1994) suggest that a plane of weakness may be created between the cover and the core by the relatively large volume of tie reinforcement used in HSC columns. These are also the current thoughts on the topic expressed by ACI-ASCE Committee 441 (1997). The FE analyses reveal, in fact, that the early cover spalling can be explained by the triaxial state of stress at the cover-core interface. Fig. 6 shows the mechanism of cover spalling whereby a crack forms between the cover shell and the core due to the restraint provided to the core by the ties. As the column is loaded axially, the Poisson growth of the core is restrained by the passive pressure provided by the ties. The cover shell is restrained however, only by the existence of a tensile stress at the cover-core interface. A cracking plane therefore forms once the tensile stress across the interface exceeds the concrete's tensile capacity in the existing triaxial state of stress.

A postanalysis of the FE results of column CC-15 shows that at the point of spalling, the minor principal stress in the concrete was $\sigma_3 = 73.5$ MPa compression and occurred approximately in the longitudinal direction. The major principal stress (approximately in the radial direction) at the core-cover interface was $\sigma_1 = 1.10$ MPa tension, and in the out-of-plane (θ) direction, the intermediate stress was $\sigma_2 = 1.52$ MPa compression. The stress state of the cover is compared in Fig. 7 against the triaxial failure surface of Menetrey and William (1995) in the plane $\sigma_2 = 0.021\sigma_3$ and for $f_{cp}/f_{tp} = 20$, where f_{cp} and f_{tp} are the in-situ compressive and tensile strengths, respectively. With $\sigma_1 = -0.015\sigma_3$, spalling occurs at a tension stress of approximately one-quarter of the uniaxial tensile

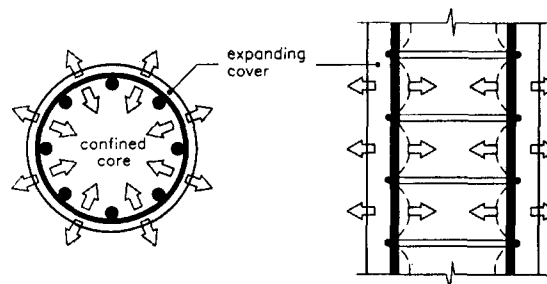


FIG. 6. Mechanics of Cover Spalling

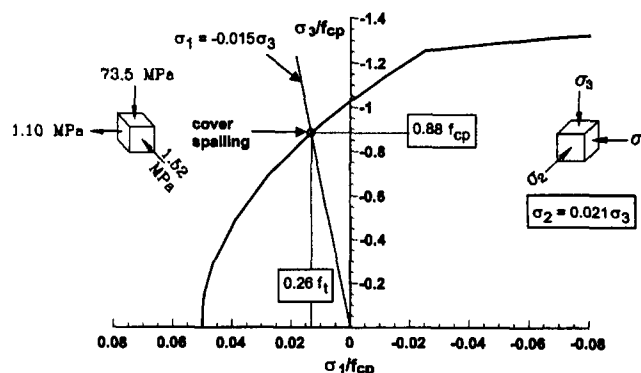


FIG. 7. Cross Section of Menetrey and William Triaxial Failure Surface at $\sigma_2 = 0.0207\sigma_3$, Showing Point of Cover Spalling for Razvi and Saatcioglu's (1996) Specimen CC-15

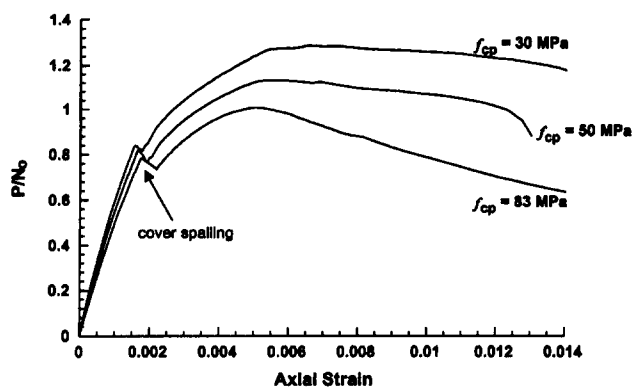


FIG. 8. Comparison of 250 mm Diameter Column, Similar to Razvi and Saatcioglu's Specimen CC-15, for Different Strengths of Concrete

strength (Fig. 7) at a compression loading corresponding to a stress of $0.88 f_{cp}$. Two other points are immediately obvious from Fig. 7. The first point is that the greater the confinement, the earlier the crack formation (relative to the squash load), explaining the observations of Cusson and Paultre (1994). The second point is the fact that tension cracks will form at the core-cover interface at a load lower than the theoretical squash load for all strengths of concrete. Once significant tension strength is lost between the cover and the core, the cover is free to buckle or spall away from the column.

Although in conventional-strength concrete columns a crack will form at the core-cover interface, the cover may not immediately spall away from the core. Tests by Sheikh and Uzumeri (1980) suggest that the cover continues to carry load after the peak compressive stress is attained. This may be due to the lower loads carried in the cover shell of conventional-strength concrete columns compared to those of HSC columns, or due to a higher residual tensile capacity after cracking. In any event, in conventional-strength columns, the load at which the cover spalls is not generally the peak load. Once the cover spalls away, significant microcracking in the core causes the core to dilate, activating the passive confining pressure of the tie reinforcement. The triaxial compressive stresses induced into the core increase its strength to well beyond the squash load. The failure loads in the Sheikh and Uzumeri columns were shown to be a function of the amount of, and arrangement of, tie reinforcement. For HSC columns, the relative increase in the peak load over the spalling load is less than that for conventional-strength columns given the same tie steel arrangements. This is demonstrated in Fig. 8, where columns of the same dimensions and reinforcement arrangements of specimen CC-15 were analyzed for concrete strengths of 30, 50, and 83 MPa. Fig. 8 shows two peaks—the first at the time of spalling, and the second as the confining pressure provided by the ties is activated. This is consistent with the experimental observations of Sheikh and Uzumeri (1980) on conventional-strength columns, and with the tests of Cusson and Paultre (1994) and Razvi and Saatcioglu (1996) on HSC columns. Experimental studies by Cusson and Paultre (1994) and Razvi and Saatcioglu (1996) show that on well-confined columns with strengths greater than 80 MPa, the second peak is approximately equal to, or lower than, the spalling peak. For these columns the maximum load is the spalling load.

EXPERIMENTAL CORROBORATION

In studies on conventional-strength concrete columns, Sheikh and Uzumeri (1980) observed that the cover carried negligible load at a strain of ϵ_{50u} , where ϵ_{50u} is the strain at which the stress drops to 50% of the ultimate in a concrete cylinder. Thus, at the first peak load the cover contributes to

the strength of the section. The second peak load occurs after the cover has spalled and the confinement provided by the tie reinforcement has been fully activated. In fact, in the well-confined specimens of Sheikh and Uzumeri a second peak is not evident; rather, a long plateau occurs at the peak load. This indicates that the cover concrete loses its load gradually while, at the same time, the passive confinement of the core is gradually activated. The loss of load carried by the cover is then taken by the core. Once the cover has spalled, the axial load is carried by the confined core. In tests on HSC columns by Cusson and Paultre (1994), it was observed that the cover spalled suddenly with a drop in load of 10–15% recorded at the time of spalling. At this point, the confining restraint provided by the ties is activated and the column may again carry increased load.

Sheikh and Uzumeri (1982) proposed a procedure to determine the stress-strain curve of confined concrete based on a conceptual model in which it was postulated that the area of the effectively confined concrete in a column is less than the core area. The effectively confined concrete was assumed to arch between the points where the lateral steel exerts a confining pressure on the concrete. In the case of rectilinear lateral reinforcement, the area of the effectively confined core is less than the core area even at the tie level, and is further reduced away from the tie level. In the case of circular lateral reinforcement, the reduction of the core area to an effectively confined area takes place only along the longitudinal axis of the column. Mander et al. (1988), Saatcioglu and Razvi (1992), and Cusson and Paultre (1995) further refined the concept advanced by Sheikh and Uzumeri (1982). In these studies, it was hypothesized that the confining pressure on the core dissipates between ties and away from longitudinal bars with the full confining pressure acting over a reduced or effective core area, A_{eff} . The core area, A_{core} , is normally defined by the enclosed area inside the perimeter of the centerlines of the outer ring of spirals or ties. The effective core area is given by

$$A_{eff} = k_e A_{core} \quad (6)$$

where k_e = confinement effectiveness coefficient ($k_e \leq 1$). The confining pressure is calculated by assuming the ties to have yielded and the equilibrating stresses on the core to be uniformly distributed. Examples of calculating the confining stress (f_r) for some common sections are shown in Fig. 9.

For circular columns with tie or spiral reinforcement, assuming a parabolic arch between the ties with a 45° tangent slope following the concept advanced by Sheikh and Uzumeri (1982), the confinement effectiveness factor is

$$k_e = \left(1 - \frac{s^*}{2d_s}\right)^2 \quad (7)$$

where s^* = clear spacing between the ties or spirals as used by Mander et al. (1988); and d_s = diameter of the tie or spiral reinforcement. For square or rectangular sections, a modified form of the Sheikh and Uzumeri (1982) model is used with the confinement effectiveness parameter given by

$$k_e = \left(1 - \frac{1}{\alpha A_{core}} \sum_{i=1}^n w_i^2\right) \times \left(1 - \frac{s^*}{2b_c}\right) \left(1 - \frac{s^*}{2d_c}\right) \quad (8)$$

where w_i = i th clear distance between adjacent tied longitudinal bars; b_c and d_c = core dimensions to the centerline of the ties across the width and depth of the section; $A_{core} = b_c d_c$; n = number of spaces between tied longitudinal bars; and α = constant, which is equal to 6 if the arches of the effectively confined concrete are assumed to have an initial tangent of 45°. Although Sheikh and Uzumeri (1982) observed that $\alpha = 5.5$ fitted their test data better, a value of $\alpha = 6$ is used in the analysis presented next.

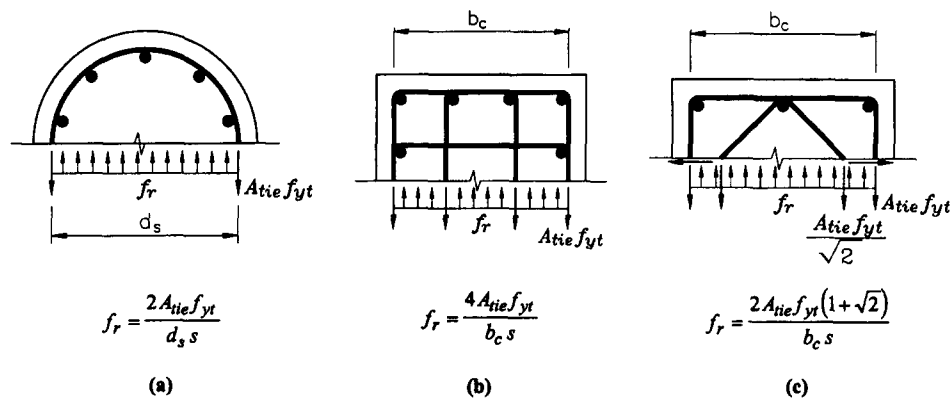


FIG. 9. Calculation of Confining Pressures for Some Common Section Types

The core strength (f_0) can be obtained by using a modified form of the Richart et al. (1929) equation

$$f_0 = f_{cp} + k_c C f_r \quad (9)$$

where f_{cp} = unconfined in-situ concrete strength; and C = confinement parameter. For the analyses that follow, the confinement parameter was taken as $C = 4$ for $f'_c \leq 80$ MPa and $C = 3$ for $f'_c > 80$ MPa, as recommended by the Federation Internationale de la Précontrainte report ("High" 1990). The capacity of the confined core including the longitudinal reinforcement is then given by

$$P_{core} = f_0(A_{core} - A_{st}) + A_{st}f_{sy} \quad (10)$$

where A_{st} = area of longitudinal tension reinforcement; and f_{sy} = yield strength of the longitudinal reinforcement.

In Fig. 10(a), the data of Sheikh and Uzumeri (1980), Toklucu and Sheikh (1992), Cusson and Paultre (1994), and Razvi and Saatcioglu (1996) have been normalized against the squash load and plotted against the cylinder strength. In Fig. 10(a), the squash load N_0 is calculated as

$$N_0 = k f'_c A_c + A_{st} f_{sy} \quad (11)$$

where f'_c = measured cylinder strength; A_c = gross area of concrete in the section; and k = factor to account for the difference in the cylinder strength to that of the in-situ concrete ($k = f_{cp}/f'_c$). Razvi and Saatcioglu (1996) measured $k \approx 0.9$, and this value was taken for all specimens compared in Fig. 10. Fig 10(a) shows that for cylinder strengths greater than 60 MPa, the peak load is approximately 0.85 times the squash load calculated by (11). This compares well with the finite-element results for Razvi and Saatcioglu's specimen CC-15, for which it was shown that spalling occurs when the concrete is stressed to approximately 0.88 times its in-situ strength. From the evidence presented, the spalling load can be taken as

$$P_{spall} = 0.85 k f'_c A_c + A_{st} f_{sy} \quad (12)$$

and the maximum capacity of the section is then obtained from

$$P_{max} = \max(P_{spall}, P_{core}) \quad (13)$$

In Fig. 10(b), the experimentally obtained peak loads are normalized against the theoretical capacity, including the longitudinal steel, as calculated using (10), (12), and (13). Fig. 10(b) indicates that for all strengths of concrete, the cover is ineffective after the initiation of the cover-core cracking. The peak load then becomes the greater of the spalling load (taken as the load corresponding to the commencement of cover-core cracking) and the capacity of the effectively confined core [as given by (13)]. Comparison of Figs. 10(a) and 10(b), however, indicates that the spalling loads are only of concern for columns with $f'_c \geq 60$ MPa.

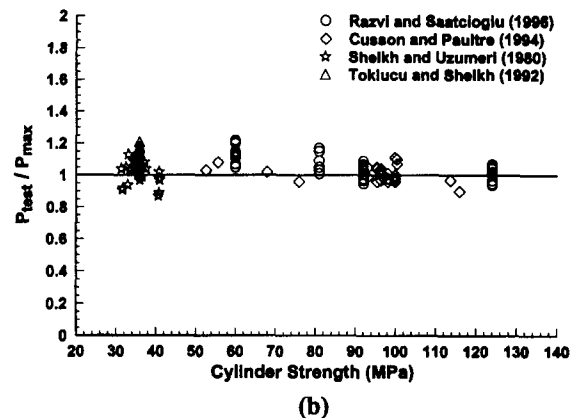
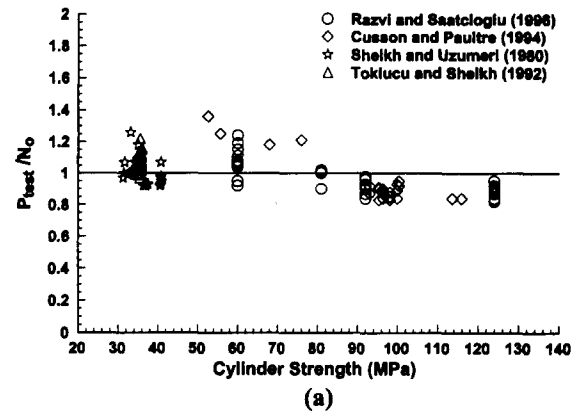


FIG. 10. Comparisons between Experimental Data Normalized against: (a) Squash Load; (b) Maximum of Confined Core Strength and Cover Spalling Load for Conventional and HSC Columns Loaded in Concentric Compression

EFFECT OF TIE YIELD STRENGTH ON AXIAL STRENGTH OF DUCTILITY

Three FE analyses were undertaken to investigate the effect of tie yield strength on the axial capacity and on the ductility of large circular HSC columns. A 2 m long section of an 800 mm diameter column was modeled with the FE mesh shown in Fig. 11. The concrete strength was taken as 83 MPa with the microplane material parameters as given by Liu and Foster (1998b) and with a 2×2 Gaussian quadrature used to generate the elemental stiffness matrix. The section of column analyzed is symmetric about the centerline and envelops the column's localization region. The section was reinforced with 2.4% of longitudinal reinforcement (equivalent to 12–36 mm diameter bars) and with 12 mm diameter tie reinforcement spaced at 100 mm centers. An elastic perfectly plastic material

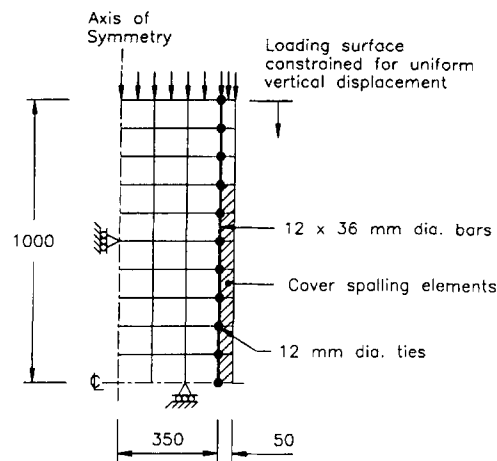


FIG. 11. FE Mesh for 800 mm Diameter Columns

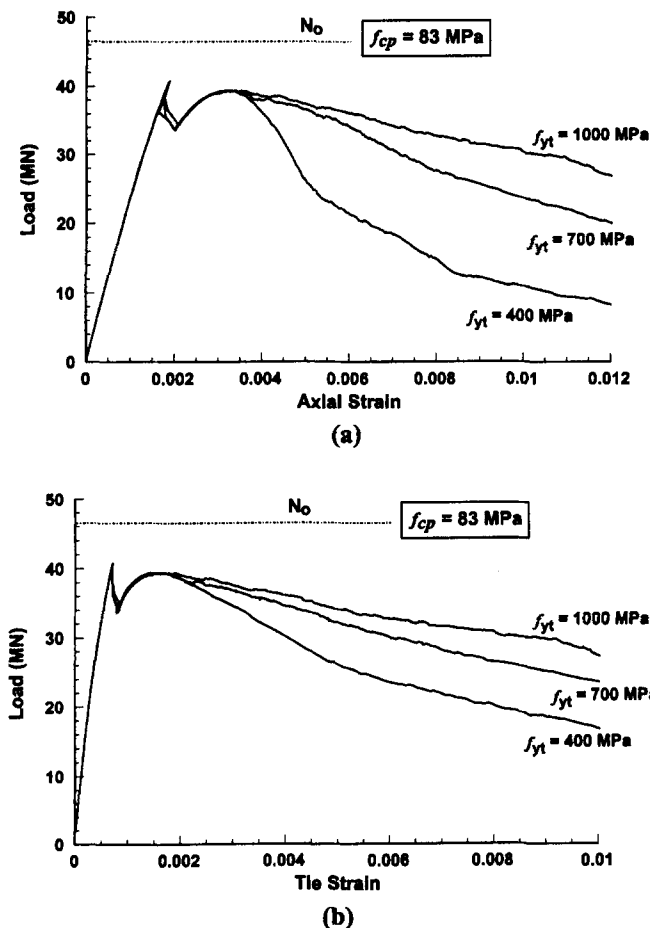


FIG. 12. Comparison of Behavior of 800 mm Diameter HSC Column with Varying Tie Yield Strengths: (a) Load versus Axial Strain Measured over Half Gauge Length of 400 mm; (b) Load versus Tensile Strain in Central Tie

model was used for the longitudinal and tie steel with a modulus of elasticity of 200 GPa. The yield strength of the longitudinal reinforcement was taken as 400 MPa, with yield strengths of 400, 700, and 1,000 MPa used for the ties. Localization about the centerline was forced by the arrangement of the cover spalling elements. The cover concrete was set to spall when it reached a radial tension strain of $750 \mu\epsilon$.

The peak load for the three analyses was 40.8 MN (88% of the squash load) and corresponded to the spalling load. Load versus strain results are shown in Fig. 12, with the axial strains calculated over a half gauge length of 400 mm measured from

the centerline. After cover spalling, the load initially decreased. As the core expands, and with increasing damage, the axial load slightly increases to a second peak of 39.4 MN, or 85% of the theoretical squash load (N_0). Once the second peak is reached, the load again decreases with increasing axial strain. While there is no improvement in the axial strength of the columns for increasing tie steel strengths, there is an improvement in ductility. Using the I_{10} ductility measure defined by Foster and Attard (1997b), where for a perfectly elastic-brittle material $I_{10} = 1$ and for an elastic perfectly plastic material $I_{10} = 10$, the I_{10} results for the columns with 400, 700, and 1,000 MPa tie steel are 5.8, 7.7, and 8.4, respectively. Thus, while increasing the strength of the tie reinforcement does not improve the column's strength, it does enhance its ductility. The early spalling of the cover also assists in obtaining the higher ductility results, giving a trade-off in strength for ductility.

CONCLUSIONS

Experimental studies on HSC columns have shown that the cover concrete may spall before the theoretical squash load is reached, if the squash load is obtained using principles developed for conventional-strength concrete. Finite-element modeling of concentrically loaded circular columns shows that a cracking plane develops at the cover-core interface when the axial stress in the concrete is less than the concrete's uniaxial compressive strength. The crack develops when the tensile stress at the cover-core interface reaches its triaxial strength limit, which is considerably below its uniaxial tension strength. Further, it is clear from the triaxial state that exists at the cover-core interface that cracking will occur at a load less than the squash load irrespective of the strength of the concrete. Once cover-core interface cracks have developed, the cover concrete is free to spall or buckle away. Analysis of experimental data on concentrically loaded square and circular columns shows that the strength of the section is limited by either the spalling load or by the capacity of the confined core. For columns with moderate to high quantities of the reinforcement, typical of HSC columns, the spalling load can be taken as 0.85 times the capacity of the concrete section (based on the in-situ concrete strength) plus the capacity of the longitudinal reinforcement.

In the present study, a large (800 mm diameter) section was analyzed to determine the effect of increasing the yield strength of the tie reinforcement on the strength and ductility of HSC columns. The analyses show that the peak strength coincided with cover spalling, with no improvement in the column's strength resulting from increasing the strength of the ties. However, significant improvements in ductility were observed with increasing tie strengths. Ductility analyses show that well-confined high-strength concrete columns with high-strength ties can achieve ductility levels comparable to those for conventional-strength concrete columns. While early cover spalling is detrimental to the strength of HSC columns, it improves the ductility when using standard ductility measurement concepts. That is, the trade-off in strength is improved ductility.

ACKNOWLEDGMENTS

The work reported in the present study was undertaken while the first writer was on special studies leave at the University of Toronto, Canada. The assistance of the staff of the Department of Civil Engineering, and the provision by the department of the resources necessary to complete this work are gratefully acknowledged.

APPENDIX. REFERENCES

- ACI-ASCE Committee 441. (1997). "High strength concrete columns: State of the art." *ACI Struct. J.*, 94(3), 323–335.

- Bažant, Z. P., and Prat, P. C. (1988a). "Microplane model for brittle-plastic material. I: Theory." *J. Engrg. Mech.*, ASCE, 114(10), 1672–1688.
- Bažant, Z. P., and Prat, P. C. (1988a). "Microplane model for brittle-plastic material. II: Verification." *J. Engrg. Mech.*, ASCE, 114(10), 1689–1702.
- Bažant, Z. P., Xiang, Y., and Prat, P. C. (1996). "Microplane model for concrete. II: Data delocalization and verification." *J. Engrg. Mech.*, ASCE, 122(3), 255–262.
- Carol, I., Prat, P. C., and Bažant, Z. P. (1992). "New explicit microplane model for concrete: Theoretical aspects and numerical implementation." *Int. J. Solids and Struct.*, 29(9), 1173–1191.
- Collins, M. P., Mitchell, D., and MacGregor, J. G. (1993). "Structural design considerations for high-strength concrete." *Concrete Int.* (May), 27–34.
- Cusson, D., and Paultre, P. (1994). "High strength concrete columns confined by rectangular ties." *J. Struct. Engrg.*, ASCE, 120(3), 783–804.
- Cusson, D., and Paultre, P. (1995). "Stress-strain model for confined high-strength concrete." *J. Struct. Engrg.*, ASCE, 121(3), 468–477.
- Foster, S. J., and Attard, M. M. (1997a). "Ductility and strength in HSC columns." *1st Engrg. Found. Conf. on High Strength Concrete* (in press).
- Foster, S. J., and Attard, M. M. (1997b). "Experimental tests on eccentrically loaded high strength concrete columns." *ACI Struct. J.*, 94(3), 2295–2303.
- "High strength concrete—State of the art report." (1990). Federation Internationale de la Précontrainte, London.
- Liu, J., and Foster, S. J. (1998a). "A finite model to study the behavior of confined concrete columns." *J. Struct. Engrg.*, ASCE, 124(9), 1011–1017.
- Liu, J., and Foster, S. J. (1998b). "Microplane model for the finite element analysis of reinforced concrete tied columns." *UNICIV Rep. R-368*, School of Civ. and Envir. Engrg., The Univ. of New South Wales, Sydney, Australia.
- Mander, J. B., Priestley, M. J. N., and Park, R. (1988). "Theoretical stress-strain model for confined concrete." *J. Struct. Engrg.*, ASCE, 114(8), 1804–1825.
- Menetrey, P., and William, K. J. (1995). "Triaxial failure criterion for concrete and its generalization." *ACI Struct. J.*, 92(3), 311–318.
- Paultre, P., Khayat, K. H., Langlois, Y., Trudel, A., and Cusson, D. (1996). "Structural performance of some special concretes." *4th Int. Symp. on Utilization of High-Strength/High-Perf. Concrete*, Presses de l'École Nationale des Ponts et Chaussées, Paris, 787–796.
- Polat, M. B. (1992). "Behaviour of normal and high strength concrete under axial compression," Master of Applied Science thesis, Dept. of Civ. Engrg., Univ. of Toronto, Canada.
- Razvi, S. R., and Saatcioglu, M. (1996). "Tests of high strength concrete columns under concentric loading." *Rep. OCEERC 96-03*, Dept. of Civ. Engrg., Univ. of Ottawa, Canada.
- Richart, F. E., Brandtzaeg, A., and Brown, R. L. (1929). "The failure of plain and spirally reinforced concrete in compression." *Bull. 190*, Univ. of Illinois, Engrg. Experimental Station, Champaign, Ill.
- Saatcioglu, M., and Razvi, S. R. (1992). "Strength and ductility of confined concrete." *J. Struct. Engrg.*, ASCE, 118(6), 1590–1607.
- Sheikh, S. A., and Uzumeri, S. M. (1980). "Strength and ductility of tied concrete columns." *J. Struct. Engrg.*, ASCE, 106(5), 1079–1102.
- Sheikh, S. A., and Uzumeri, S. M. (1982). "Analytical model for concrete confinement in tied columns." *J. Struct. Engrg.*, ASCE, 108(12), 2703–2722.
- Sundaraj, P., and Sheikh, S. A. (1992). "High strength concrete columns under eccentric loads." *Res. Rep.*, Dept. of Civ. Engrg., Univ. of Toronto, Canada.
- Toklucu, M. T., and Sheikh, S. A. (1992). "Behaviour of reinforced concrete columns with circular spirals and hoops." *Res. Rep.*, Dept. of Civ. Engrg., Univ. of Toronto, Canada.
- van Mier, J. G. M. (1997). *Fracture processes of concrete: Assessment of material parameters for fracture models*. CRC Press, Inc., Boca Raton, Fla.